Fluidized-Bed Combustion of Biomass with Elevated Alkali Content: A Comparative Study between Two Alternative Bed Materials

P. Ninduangdee, V. I. Kuprianov

Abstract—Palm kernel shell is an important bioenergy resource in Thailand. However, due to elevated alkali content in biomass ash, this oil palm residue shows high tendency to bed agglomeration in a fluidized-bed combustion system using conventional bed material (silica sand). In this study, palm kernel shell was burned in the conical fluidized-bed combustor (FBC) using alumina and dolomite as alternative bed materials to prevent bed agglomeration. For each bed material, the combustion tests were performed at 45kg/h fuel feed rate with excess air within 20–80%. Experimental results revealed rather weak effects of the bed material type but substantial influence of excess air on the behaviors of temperature, O_2, CO, C_xH_y, and NO inside the reactor, as well as on the combustion efficiency and major gaseous emissions of the conical FBC. The optimal level of excess air ensuring high combustion efficiency (about 98.5%) and acceptable level of the emissions was found to be about 40% when using alumina and 60% with dolomite. By using these alternative bed materials, bed agglomeration can be prevented when burning the shell in the proposed combustor. However, the two bed materials exhibited significant changes in their morphological, physical and chemical properties in the course of the time.

Keywords—Palm kernel shell, fluidized-bed combustion, alternative bed materials, combustion and emission performance, bed agglomeration prevention.

I. INTRODUCTION

PALM oil industry is an important industrial sector in the Thai economy. Presently, the oil palm plantation area in Thailand accounts for about 4.1 million rais (or 656,000 hectares) ensuring production of about 12 million tons of fresh fruit bunches per year [1]. During palm oil processing, a tremendous quantity of oil palm residues (such as empty fruit bunches, palm kernel shell, fiber, fronds and leaves), equivalent to some 100 PJ energy, are annually produced in the country [2]. Development and study of reliable, high-efficiency and environmentally-friendly systems for utilization of these bioresources with great energy potential is an issue of paramount importance for national energy-related sectors.

The fluidized-bed combustion technology is proven to be one of the most effective and environmental friendly technologies for energy conversion from various agricultural and forest-related residues [3], [4]. However, the combustion of biomass with high/elevated alkali metal contents in a fluidized-bed system using conventional bed material (silica sand) is often accompanied by some undesirable ash-related processes, such bed sintering and agglomeration. Reactions of alkali compounds (vaporized from biomass ash) with SiO_2 on the surface of silica grains result in formation of a sticky alkali-silicate (surface) layer basically regarded to be a primary cause of bed agglomeration [3], [5]–[7].

During the fluidized-bed combustion of oil palm residues with their elevated/high potassium contents in biomass ash, a risk of bed agglomeration is expected to be high [8], [9]. To prevent this undesirable phenomenon, various alternative bed materials, such as alumina, aluminum-rich materials, dolomite, and limestone, can be used to ensure reliable operation of fluidized-bed combustion techniques fired such residues [3], [5], [10], [11].

A fluidized-bed combustor with a cone-shape bed (referred to as 'conical FBC') seems to be a suitable fluidized-bed combustion technique for testing new (alternative) bed materials [10], particularly those of relatively high cost. Compared to a columnar fluidized-bed combustion system (combustor/furnace) for burning biomass, the conical FBC is characterized by a lower pressure drop across the fluidized bed, shorter start-up time, and uniform cross-sectional distribution of combustion characteristics [4], [12].

This work was aimed at investigating the feasibility of high-efficiency and safe burning of palm kernel shell in the conical FBC using two alternative bed materials – alumina and dolomite – for a wide range of excess air, a key operating parameter. The effects of both excess air and bed material type on combustion and emission performance of the combustor were the focus of this study. To investigate behavior and condition of the bed materials in the course of the time, the particle size distribution and composition of the materials were analyzed for different operating times.

II. MATERIALS AND METHODS

A. Experimental Set Up

Fig. 1 shows the schematic diagram of an experimental set up with the conical FBC. The combustor consisted of two steel sections assembled coaxially: (1) a conical section of 0.9m height with 40° cone angle and 0.25m inner diameter at the bottom plane, and (2) a cylindrical section comprising five cylindrical modules of 0.5m height and 0.9m inner diameter. Both sections had 4.5-mm thick metal walls lined internally with the 50-mm thick refractory-cement insulation.

P. Ninduangdee and V.I. Kuprianov are with School of Manufacturing Systems and Mechanical Engineering, Sirindhorn International Institute of Technology, Thammasat University, P.O. Box 22, Thammasat Rangsit Post Office, Pathum Thani 12121, Thailand (e-mail: ivlaanov@siit.tu.ac.th).
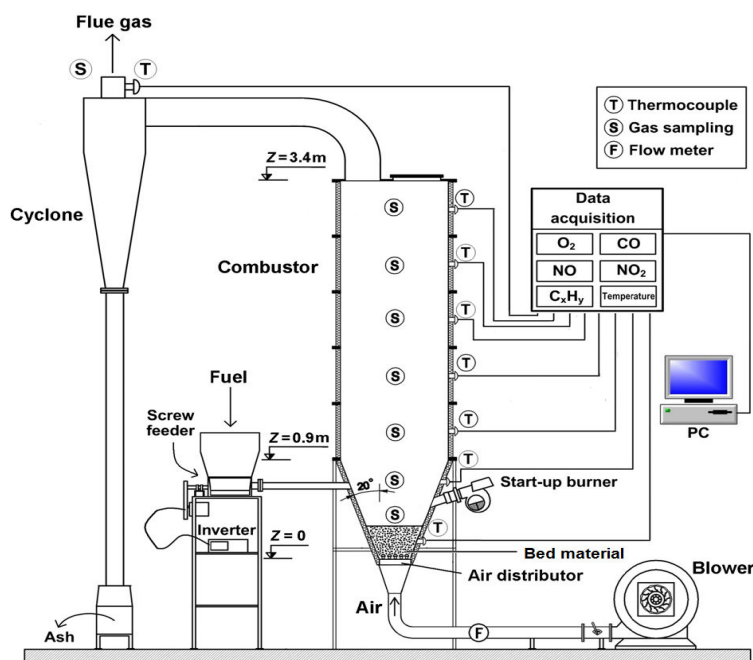
Fig. 1 Schematic diagram of an experimental set up with the conical FBC

Besides the combustor, the experimental set up included a startup burner fired with diesel oil fuel, a screw-type fuel feeder, a 25-hp blower supplying air to the reactor, a cyclone collecting particulates from the flue gas leaving the combustor, as well as various facilities and instruments for measurement, acquisition and treatment of experimental data.

The blower delivered air to the combustor through an air pipe of 0.1m inner diameter. Air was injected into the sand bed through an air distributor with nineteen bubble caps arranged at the bottom plane of the conical module. The air distributor was employed to generate a fluidized bed in the conical section of the reactor ensuring uniform distribution of airflow over the bed at an insignificant pressure drop across the distributor.

To measure temperature and gas concentrations (O_2, CO, C_xH_y as CH_4, and NO) inside the reactor, the conical FBC was equipped with stationary Chromel-Alumel thermocouples (of type K) and gas sampling ports located at different levels along the combustor height as well as at the cyclone exit, as shown in Fig. 1.

B. The Fuel

Table I shows the proximate and ultimate analyses, the composition of fuel ash, as well as the lower heating value of palm kernel shell used in this study. As found in setting tests, the hard structure of the shell caused serious problems in stable feeding of this biomass to the reactor. To achieve high combustion efficiency and steady operation of the combustor, palm kernel shell was shredded prior to combustion tests. After shredding, the size of the shredded palm kernel shell was quite irregular, ranging from 0.1mm (exhibiting dust-like appearance) to 9mm.

TABLE I
PROPERTIES OF PALM KERNEL SHELL USED IN THE COMBUSTION STUDY

Property	Palm kernel shell
Proximate analysis (on as-received basis, wt.%)	
Moisture	5.4
Volatile matter	71.1
Fixed carbon	18.8
Ash	4.7
Moisture	5.4
Ultimate analysis (on as-received basis, wt.%)	
C	48.06
H	6.38
N	1.27
O	34.10
S	0.09
Ash composition (as oxides, wt.%)	
SiO_2	54.1
Al_2O_3	3.1
K_2O	8.1
CaO	23.2
Na_2O	0.8
MgO	2.7
Fe_2O_3	6.1
P_2O_5	1.2
Lower heating value (kJ/kg)	16,300

It can be seen in Table I that the selected biomass had quite significant content of volatile matter, a moderate proportion of fixed carbon, but rather low contents of fuel moisture and fuel ash. Due to rather low fuel S, SO_2 was not addressed in this study.

The standard analysis of fuel ash (wt.%, as oxides) exhibited a predominant proportion of silicon (SiO_2 = 54.1%), followed by calcium (CaO = 23.2%), potassium (K_2O = 8.1%) and iron (Fe_2O_3 = 6.1%). The elevated potassium content in the fuel ash indicated a potential problem (bed agglomeration)

during the combustion of this biomass in a fluidized bed when using conventional bed material (silica sand).

TABLE II
COMPOSITION OF THE BED MATERIALS USED IN THE CONICAL FBC

Bed material	Composition (wt.%)						
	Al_2O_3	SiO_2	CaO	MgO	K_2O	Na_2O	Fe_2O_3
Alumina sand	87.18	12.29	0.04	–	0.43	0.01	0.01
Dolomite	0.08	0.19	61.40	38.31	–	0.02	–

C. The Bed Materials

In this study two alternative bed materials, alumina sand and dolomite, both of 300–500μm in particle size, were used for preventing bed agglomeration in the combustor. The solid density of alumina and dolomite was 3500kg/m^3 and 2800 kg/m^3, respectively.

Table II shows the composition of alumina sand and dolomite quantified by using a wavelength dispersive X-ray fluorescence spectrometer. It can be seen in Table II that Al_2O_3 was the predominant component in alumina sand, whereas major elements in dolomite were calcium (CaO = 61.4 wt.%) and magnesium (MgO = 38.31 wt.%).

D. Experimental Procedure

A diesel-fired start-up burner from the Riello Burners Company (model "Press G24") was used to preheat the bed material during combustor start up. When the bed temperature reached about 700°C, a diesel pump of the burner was turned off. However, during the combustion tests, a burner fan continued its operation at the minimum airflow rate in order to protect a nozzle head of the burner from overheating. In the meantime, a rectangular 20cm x 30cm steel curtain was used to screen the burner from the combustion chamber and thus to avoid impacts by the flame and particulates onto the start-up burner.

The screw-type feeder delivered the fuel into the conical module at a level $Z = 0.6$m above the air distributor. A three-phase inverter was used to control the fuel feed rate via adjusting the rotational speed of the screw feeder.

In this study, the percentage of excess air (EA) was selected as the major operating variable. For each test run, the excess air value was quantified according to [13] using O_2, CO and C_xH_y (as CH_4) at the cyclone exit, whereas heat loss due to unburned carbon as well as that owing to incomplete combustion (both as the percentage of LHV) were predicted together with the combustion efficiency using a standard method [13]. Unburned carbon content in the fly ash was determined by a laboratory analysis with the final aim to quantify associated heat loss. However, heat loss owing to incomplete combustion was assessed using the CO and C_xH_y (as CH_4) emissions.

The used/reused bed materials and the fly ashes were sampled and analyzed for their chemical composition using the wavelength dispersive X-ray fluorescence spectrometer with the aim to discuss the ash-related issues. The analyses were performed for three operating times: 10h, 20h, and 30h. After finishing the combustion tests, the particle size distribution and average (volumetric) particle diameter of both bed materials were determined by a "Mastersizer 2000" particle size analyzer and then compared with those of the original bed material (i.e., unused alumina sand and dolomite).

III. RESULTS AND DISCUSSION

A. Behavior of Temperature and Gas Concentrations in the Conical FBC

Fig. 2 shows the axial temperature and O_2 concentration profiles in the conical FBC using alumina sand and dolomite when firing palm kernel shell at the fuel feed rate of 45 kg/h for the excess air values of about 40% and 80%. It can be seen in Fig. 2 that the temperature and O_2 concentration profiles inside the combustor for two test groups (with alumina sand and dolomite) showed similar trends.

It can be seen in Fig. 2 that in the conical module of the reactor ($Z < 0.9$ m), the temperature profiles were quasi-uniform. This fact indicated an occurrence of turbulent fluidization regime of the expanded bed ensuring excellent mixing of bed particles with chars and gases in the combustor bottom, whereas in the cylindrical section, these profiles exhibited temperature decreasing along the combustor height, likely caused by heat losses across the reactor walls. It can be further noticed in Fig. 2 that the temperature at any point in the conical section for the case of using alumina bed was somewhat higher than that for dolomite bed. However, in the cylindrical module of the combustor, the axial temperature profiles of the two bed materials were closer. From Fig. 2, with increasing the amount of excess air, temperature in all locations inside the reactor decreased, mainly due to the strengthened dilution effects from excessive air.
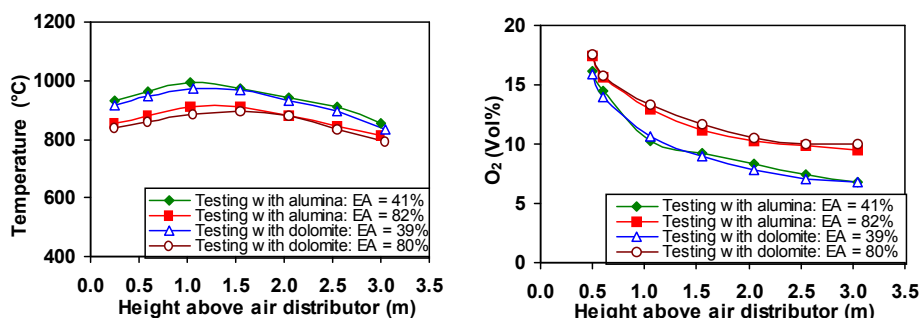
Fig. 2 Comparison of the axial temperature and O_2 profiles in the conical FBC using alumina sand and dolomite as bed materials when firing palm kernel shell at different amounts (about 40% and 80%) of excess air

Fig. 3 Comparison of the axial profiles of CO, C_xH_y, and NO in the conical FBC using alumina sand and dolomite as bed materials when firing palm kernel shell at different amounts (about 40% and 80%) of excess air
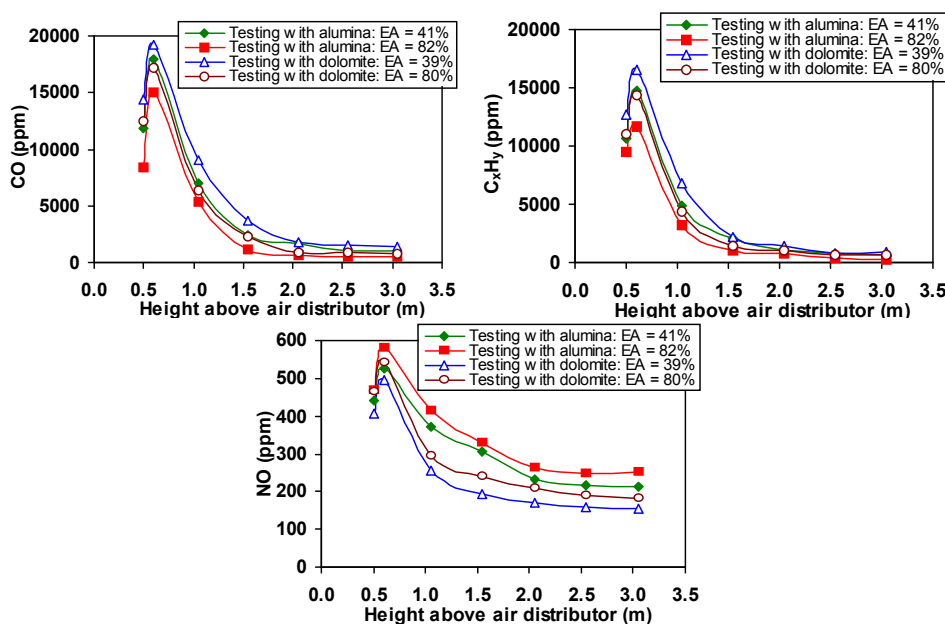
Fig. 3 compares the axial profiles of CO, C_xH_y (as CH_4), and NO inside the conical FBC between the two bed materials for operating conditions as in Fig. 2. As seen in Fig. 3, the axial CO, C_xH_y, and NO concentration profiles for both bed materials revealed two specific regions in the reactor – the bottom region ($0 < Z < 0.6$m) and the upper region ($Z > 0.6$m) – with different net results of (i) pollutants formation, (ii) CO and C_xH_y oxidation, and (iii) NO reduction.

In the first region, below the level of fuel injection ($0 < Z < 0.6$ m), both CO and C_xH_y showed a significant increase along the axial direction, mainly due to the rapid devolatilization of biomass, followed by oxidation of CO and C_xH_y, and fuel chars. However, due to increased bed temperature (see Fig. 2), the oxidation rate of CO and C_xH_y for the case with alumina sand was higher, which resulted in lower peaks of these pollutants (at $Z \approx 0.6$m) compared to those when using dolomite. For the two bed materials, switching the combustor to firing the biomass at higher excess air led to substantially lower peaks of CO and C_xH_y, and this was likely caused by the

higher oxidation rate of the carbonaceous compounds in the first region.

In the second region ($Z > 0.6$m), where the secondary (oxidation) reactions were predominant, both CO and C_xH_y showed a diminishing trend along the combustor height. A decrease of CO along the combustor height was mainly due to oxidation of CO by O_2 and OH [14], whereas the C_xH_y oxidation process involved two groups of secondary reactions: (i) breakdown of C_xH_y to CO, and, afterwards, (ii) oxidation of CO to CO_2 [14].

As known, during biomass combustion, NO is basically formed from volatile nitrogenous species (mainly, NH_3) through the fuel-NO formation mechanism including the proportional effects of fuel N, temperature and excess air [3], [14]. However, due to secondary reactions, such as catalytic reduction of NO by CO on a surface of char, ash, and bed material particles, as well as homogeneous reactions of NO with C_xH_y, may lead to a substantial decrease of the produced NO at different points.

Like CO and C_xH_y, the axial NO concentration profiles showed two specific regions. In the first region ($0 < Z < 0.6$ m), NO increased rapidly along the combustor height in all the test runs with the two bed materials, as the rate of NO formation in this region was significantly higher than that of NO reduction. It can be seen in Fig. 3 that the rate of NO formation and, consequently, the NO peak observed in the vicinity of biomass injection (i.e., at $Z \approx 0.6$ m) were substantially higher in the tests with alumina (for similar values of excess air). This result can be explained by the higher bed temperature and lower peak of CO in the vicinity of fuel injection. In the meantime, the rate of NO formation in this region and, accordingly, the NO peak were higher at higher excess air (according to the above fuel-NO formation mechanism).

In the second region of the reactor ($Z > 0.6$ m), the rate of the chemical reactions responsible for NO reduction prevailed the formation rate of NO, and this resulted in a substantial decrease of NO along the combustor height. In the tests with alumina sand, the reduction rate of NO was substantially lower than that for the tests with sand-like dolomite, mainly due to the lower CO and C_xH_y concentrations at different points in this region.

B. Emissions and Combustion Efficiency of the Combustor

Table III summarizes the dependent variables – unburned carbon content in the fly ash, emissions of CO, C_xH_y (as CH_4), and NO from the combustor (all on a dry gas basis and at 6% O_2) together with combustion-related heat losses and combustion efficiency of the conical FBC – for the tests with distinct bed materials at actual operating conditions (excess air, and O_2 at stack).

When firing palm kernel shell at excess air of 40–80%, the major gaseous emissions (subject to control) can be ensured at levels below the national emission limits (740 ppm for CO, and 205 ppm for NO, both on a gas basis and at 6% O_2) [15], whereas the combustion efficiency was basically high, within 98.6–99.2%. It can be seen in Table III that the CO and C_xH_y emissions were effectively diminished by increasing the amount excess air; whereas the NO emission was minimized via decreasing this operating variable.

Because of the insignificant ash content in palm kernel shell (see Table I) and rather low content of unburned carbon in the fly ash, the heat loss due to unburned carbon had minor effects on the heat balance of the combustor, showing, however, some decrease with increasing excess air. Hence, the combustion efficiency was mainly influenced by the heat loss due to incomplete combustion, which followed the behavior of the CO and C_xH_y emissions. From Table III, the combustion efficiency can be generally improved by increasing excess air, however to an insignificant extent, as follows from data for excess air of 40–80%.

TABLE III
EMISSIONS, HEAT LOSSES, AND COMBUSTION EFFICIENCY OF THE CONICAL FBC USING ALUMINA AND DOLOMITE AS THE BED MATERIALS DURING COMBUSTION OF PALM KERNEL SHELL AT 45 KG/H AT VARIABLE EXCESS AIR

Excess air (%)	O_2 at the cyclone exit (vol.%)	Unburned carbon in fly ash (wt.%)	Emission [a] (ppm)			Heat loss (%) due to:		Combustion efficiency (%)
			CO	C_xH_y	NO	unburned carbon	Incomplete combustion	
Test runs with alumina as the bed material								
19	3.7	4.58	1563	1330	99	0.45	1.98	97.6
41	6.2	3.09	641	561	132	0.30	1.13	98.6
60	8.0	2.79	474	431	141	0.27	1.14	98.6
82	9.5	2.27	275	228	148	0.22	0.79	99.0
Test runs with dolomite as the bed material								
19	3.8	8.76	2207	1812	115	0.91	2.76	96.3
39	6.2	7.33	1040	880	128	0.75	1.82	97.4
58	7.8	4.34	476	361	136	0.43	1.00	98.7
80	9.4	2.17	256	162	142	0.21	0.62	99.2

[a] At 6% O_2 (on a dry gas basis).
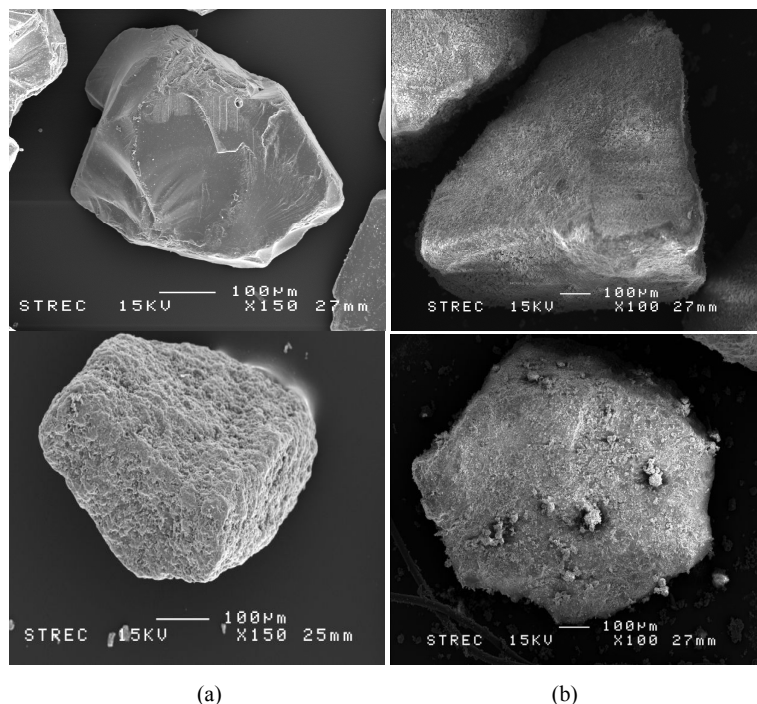
(a)   (b)

Fig. 4 SEM images of grains of the original bed materials (upper images) and those of the (re-)used bed materials (lower images) when using: (a) alumina sand and (b) dolomite
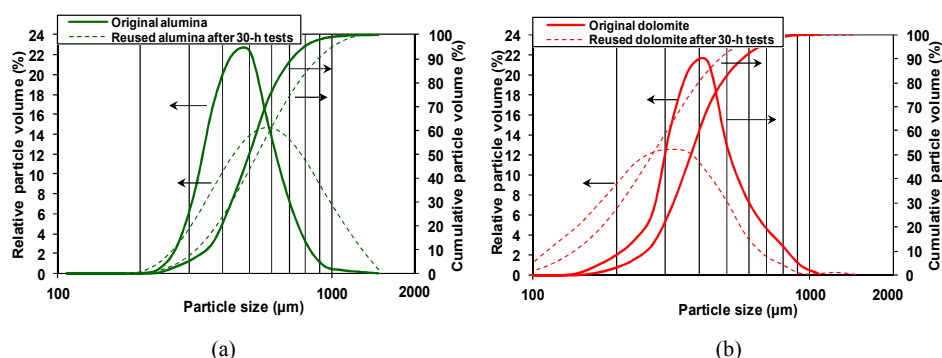

(a)   (b)

Fig. 5 Particle size distribution of the original bed material and that of the reused bed material after 30-h tests on the conical FBC for firing palm kernel shell when using: (a) alumina and (b) dolomite

To diminish the environmental impacts of NO_x (a more harmful pollutant compared to CO and C_xH_y) as well as the potential heat loss with waste gas of a boiler integrated with the proposed combustor, it can be suggested that the amount of excess air be selected at a minimum possible level ensuring, however, the CO emission from the conical FBC within the above-mentioned emission limit for this pollutant.

Based on such an approach, excess air of about 40% seems to be the best option for firing palm kernel shell in the conical FBC using alumina as the bed material, whereas excess air of about 60% is more appropriate for dolomite. Under these conditions, the conical FBC can be operated with high (~99%) combustion efficiency, while controlling the major gaseous (CO and NO) emissions within the above-mentioned national emission limits and maintaining the C_xH_y emissions at a reasonable level.

C. Time-Related Effects on the Morphology and Particle Size Distribution of the Bed Material

As revealed by a visual inspection of the bed material after completing the combustion tests with alumina sand or dolomite (for about 30h, for each material), no features of bed agglomeration were observed in the combustor.

Fig. 4 depicts the SEM micrographs of original alumina and dolomite particles (grains), as well as those after 30-h combustor testing. The SEM image of the original alumina grain revealed a quite smooth surface, whereas the surface of the dolomite particle exhibited some roughness. However, after 30-h combustor operation, an external surface of alumina grains showed an apparent roughness (clearly seen in Fig. 4)

indicating the formation of a quite thin coating layer on the grain surface (to be discussed below). When using dolomite, $CaMg(CO_3)_2$, as the bed material, the bed particles were subject to calcination, i.e., dolomite breakdown, which led to (i) appearance of fine particles mainly containing CaO and MgO and (ii) a decrease of bed particle size. As a result, fine particles from the bed calcination adhered to the grains of the reused dolomite, as can be seen in Fig. 4.

Fig. 5 shows the particle size distribution (as the volume percentage of particles for different size groups) of original alumina sand and dolomite, and that of the reused bed materials after 30h combustion tests. Apparently, the reused alumina showed an increase in the mean volumetric diameter of the bed particles compared to that of the original alumina sand, basically caused by the above-mentioned coating on the surface of bed particles [16]. The coating layer likely consisted of some eutectics (e.g. K_2O–Al_2O_3–SiO_2) characterized by high fusion temperature, basically ranged within 1500–1600 °C [17]. Due to the high fusion temperature (significantly higher than the bed temperatures observed in the conical FBC), bed agglomeration in this combustor was prevented. Unlike with alumina sand, the particle size distribution of reused dolomite showed a time-related decrease in (mean) volumetric diameter of bed particles, thus indicating the continuous attrition/breakage of the bed particles following the above-mentioned bed calcination.

However, as follows from the analysis of the size distribution in Fig. 5, the predominant proportion of the two reused bed materials was represented by the Geldart-B particles, which indicated sustainable fluidized-bed regime of the combustor for the entire experimental time.

D. Time-Related Changes in the Composition of the Bed Material and Fly Ash

Table IV shows the composition of the bed materials used/reused in the conical FBC and that of the fly ashes originated from fluidized-bed combustion of palm kernel shell at different time instants of combustor operation. As revealed by data in Table IV, the content of SiO_2, CaO and K_2O in the two bed materials increased with time, however to different extents.

Due to the collisions and attrition of alumina particles, the particle coating was destructed resulting in generation of some fine particles (containing Al) in the fluidized bed, which was consequently carried out from the bed region and became a part of fly ash. These processes explain a reduction of Al_2O_3 content in the reused bed material (roughly, by 50% for the entire experimental time), whereas the total weight of the bed remained almost constant due to absorption of ash-related particle by the bed material [16]. In the meantime, these processes made Al_2O_3 content in the fly ash substantially higher compared to that in the fuel ash (see Table II). The continuous carryover of Al_2O_3 from the bed likely led to a weakening capability of the alumina-based bed material to withstand bed agglomeration with time.

TABLE IV
COMPOSITION OF THE BED MATERIALS USED/REUSED IN THE CONICAL FBC AND THAT OF THE FLY ASHES ORIGINATED FROM THE COMBUSTION OF PALM KERNEL SHELL AT DIFFERENT TIME INSTANTS OF COMBUSTOR OPERATION

Operating time (h)	Composition (wt.%)									
	Al_2O_3	SiO_2	CaO	MgO	Na_2O	K_2O	Fe_2O_3	P_2O_5	Cl	ZnO
Bed material from the tests with alumina										
10 (used alumina)	65.1	25.32	2.57	0.65	0.47	3.68	0.34	0.21	–	0.01
20 (reused alumina)	60.42	31.24	2.66	0.61	0.33	4.25	0.33	0.13	–	–
30 (reused alumina)	51.21	35.21	3.21	0.72	0.38	5.38	0.41	0.27	–	–
Bed material from the tests with dolomite										
10 (used dolomite)	0.09	4.1	66.87	27.3	0.1	1.16	0.36	–	0.01	–
20 (reused dolomite)	0.08	5.96	66.42	25.44	0.15	2.24	0.72	–	0	–
30 (reused dolomite)	0.10	6.23	67.25	23.37	0.14	2.25	0.65	–	0	–
Fly ash from the tests with alumina										
10	15.24	48.24	21.44	1.35	0.69	6.66	3.21	1.02	–	0.01
20	8.56	52.65	22.32	2.13	0.52	5.32	2.14	1.33	–	0.01
30	8.24	52.09	23.65	2.2	0.66	4.23	2.05	1.37	–	–
Fly ash from the tests with dolomite										
10	2.81	53.5	28.3	4.15	0.96	6.21	1.12	–	0.01	0.01
20	2.8	52.1	31.15	5.21	0.93	6.32	1.32	–	0.04	0.01
30	1.98	48.31	34.64	6.11	0.87	5.14	1.14	–	0.01	0.03

The above-mentioned calcination and attrition/breakage of dolomite had significant effects on the composition of the (reused) bed material and that of the fly ash when this bed material was used in the combustor. From Table IV, these processes led to a substantial increase of CaO and MgO in the fly ash originated from the combustion of palm kernel shell. In the meantime, due to quite intensive chemical interaction between the bed material and biomass ash, the contents of silicon (SiO_2) and potassium (K_2O) in the bed material samples became significantly greater compared to original dolomite.

It should be also noted that the attrition and breakage of the

calcined dolomite into fine powder led to a sensible carryover of the bed material from the reactor and consequently resulted in a decrease of the bed material weight. To secure proper hydrodynamic characteristics of the bed, some proportion of fresh dolomite was added to the reused bed material after each 10h of combustor operation.

IV. CONCLUSIONS

The conical fluidized-bed combustor has been successfully tested for burning palm kernel shell at fuel feed rate of 45 kg/h, while ranging excess air from 20% to 80%. The use of alumina sand or dolomite as the bed material ensures safe and effective utilization of palm kernel shell with elevated potassium content in fuel ash for energy conversion via direct combustion in this technique.

Excess air has important effects on formation and oxidation/reduction of major gaseous pollutants in the reactor, as well as on combustion efficiency and emission performance of the proposed combustion technique, whereas the influence of bed material type on these processes and characteristics is rather weak. Excess air of about 40% seems to be the best option for firing palm kernel shell in the conical FBC using alumina as the bed material, whereas excess air of about 60% is more appropriate for dolomite. Combustion efficiency of about 98.5% is achievable when firing this biomass at the recommended excess air values, while controlling CO and NO emissions from the combustor at acceptable levels (meeting the national emission limits) and maintaining the C_xH_y emissions at a reasonable level.

By using alumina or dolomite as the bed material, bed agglomeration can be prevented when burning palm kernel shell with elevated potassium content in fuel ash in this conical fluidized-bed combustor.

However, due to continuous carryover of small proportion of alumina from the combustor with the fly ash, physical and chemical properties of the (reused) bed material exhibit substantial time-domain changes, thus pointing at a weakening capability of the bed to withstand bed agglomeration with time.

When using dolomite as the bed material, attrition and breakage of part of calcined dolomite into fine particles in the fluidized bed lead to a carryover of some part of the bed material from the reactor, and consequently lead to a gradual decrease of the bed weight with time. A corresponding proportion of fresh dolomite is therefore required to provide a continuous substitution of the lost bed material for sustaining desired hydrodynamic regime characteristics of the conical fluidized bed.

ACKNOWLEDGMENTS

REFERENCES

[1] Office of Agricultural Economics. Agricultural production in Thailand. http://www.oae.go.th/download/prcai/farmcrop/palm52-54.pdf.

[2] Department of Alternative Energy Development and Efficiency. Thailand Alternative Energy Situation 2012. http://www.dede.go.th

[3] J. Werther, M. Saenger, E.U. Hartge, T. Ogada, and Z. Siagi, "Combustion of agricultural residues", *Progress in Energy and Combustion Science*, vol. 26, pp. 1–27, 2000.

[4] W. Permchart and V.I. Kouprianov, "Emission performance and combustion efficiency of a conical fluidized-bed combustor firing various biomass fuels", *Bioresource Technology*, vol. 92, pp. 83–91, 2004.

[5] A.A. Khan, W. de Jong, P.J. Jansens, and H.Spliethoff, "Biomass combustion in fluidized bed boilers: Potential problems and remedies", *Fuel Processing Technology*, vol. 90, pp. 21–50, 2009.

[6] M. Öhman, A. Nordin, B.J. Skrifvars, R. Backman, and M. Hupa, "Bed agglomeration characteristics during fluidized bed combustion of biomass fuels", *Energy & Fuels*, vol. 14, pp. 169–178, 2000.

[7] W. Lin, K. Dam-Johanse, and F. Frandsen, "Agglomeration in bio-fuel fired fluidized bed combustors", *Chemical Engineering Journal*, vol. 96, pp. 171–185, 2003.

[8] P. Chaivatamaset, P. Sricharoon, and S. Tia, "Bed agglomeration characteristics of palm shell and corncob combustion in fluidized bed," *Applied Thermal Engineering*, vol. 31, pp. 2916–2927, 2011.

[9] P. Chaivatamaset, P. Sricharoon, S. Tia, and B. Bilitewski, "A prediction of defluidization time in biomass fired fluidized bed combustion", *Applied Thermal Engineering*, vol. 50, pp. 722–731, 2013.

[10] V.I. Kuprianov and P. Arromdee, "Combustion of peanut and tamarind shell in a conical fluidized-bed combustor: A comparative study", *Bioresource Technology*, vol. 140, pp. 199–210, 2013.

[11] L.M.J. Fernández, C.R. Escalada, L.J.M. Murillo, and G.J.E. Carrasco, "Combustion in bubbling fluidised bed with bed material of limestone to reduce the biomass ash agglomeration and sintering", *Fuel*, vol. 85, pp. 2081–2092, 2006.

[12] V.I. Kouprianov and W. Permchart, "Emission from a conical FBC fired with a biomass fuel", *Applied Energy*, vol. 74, pp. 383–392, 2003.

[13] P. Basu, K.F. Cen, L. Jestin, *Boilers and Burners*, Springer, New York, 2000.

[14] S. Turns, *An Introduction to Combustion*, McGraw-Hill, Boston, 2006.

[15] Pollution Control Department, Ministry of Natural Resources and Environment of Thailand. Air Pollution Standards for Industrial Sources. http://www.pcd.go.th/info_serv/reg_std_airsnd03.html.

[16] P. Ninduangdee and V. I. Kuprianov, "Study on burning oil palm kernel shell in a conical fluidized-bed combustor using alumina as the bed material", *Journal of the Taiwan Institute of Chemical Engineers*, vol. 44, pp. 1045–1053, 2013.

[17] S. Konsomboon, S. Pipatmanomai, T. Madhiyanon, and S. Tia, "Effect of kaolin addition on ash characteristics of palm empty fruit bunch (EFB) upon combustion", *Applied Energy*, vol. 88, pp. 298–305, 2011.